Sensors & Actuators: B. Chemical 424 (2025) 136905

Contents lists available at ScienceDirect

Sensors and Actuators: B. Chemical

journal homepage: www.elsevier.com/locate/snb

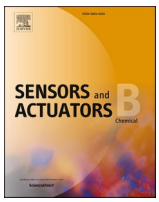

Multi-quenching electrochemiluminescence system based on resonance energy transfer from self-enhanced Ce(III, IV)-MOF@Ru to CuO@PDA@AuNPs for ultrasensitive detection of HER2

Hongying Jia [a], Nuo Zhang [a], Yuyang Li [a], Hongmin Ma [a], Dan Wu [a], Xuejing Liu [a,*], Huangxian Ju [a], Qin Wei [a,b,**]

[a] Collaborative Innovation Center for Green Chemical Manufacturing and Accurate Detection, School of Chemistry and Chemical Engineering, University of Jinan, Jinan 250022, PR China

[b] Department of Chemistry, Sungkyunkwan University, Suwon 16419, Republic of Korea

ARTICLE INFO

Keywords:
Electrochemiluminescence
Immunosensing
Resonance-energy-transfer
Self-enhanced
HER2

ABSTRACT

This study presents an innovative approach based on electrochemiluminescence resonance energy transfer (ECL-RET) through the introduction of a new pattern donor-acceptor couple. The donor of self-enhanced Ce(III, IV)-MOF@Ru is created by immobilizing $Ru(bpy)_3^{2+}$ on Ce-based metal-organic frameworks (Ce(III, IV)-MOF). The acceptor of CuO@PDA@AuNPs is the CuO nanospheres polydopamine (PDA) framework grafted with gold nanoparticles (AuNPs). An ultrasensitive detection of human epidermal growth factor receptor-2 (HER2) was achieved through the development of a quenched ECL immunosensor. Ce(III, IV)-MOF, a unique 3D infinite extension framework, was recognized for its excellent nanostructure and remarkable capacity to greatly activate tripropylamine (TPrA) and generate abundant radicals. Fortunately, it was simultaneously utilized as a highly effective coreactant accelerator and encapsulation agent, thereby facilitating the immobilization of $Ru(bpy)_3^{2+}$ and the generation of radicals for creating a self-enhanced emitter of Ce(III, IV)-MOF@Ru. Consequently, by effectively reducing the distance of electron transmission and minimizing the loss of energy, Ce(III, IV)-MOF@Ru achieved a significantly high efficiency in ECL. More importantly, CuO@PDA@AuNPs was prepared as a perfect quenching agent. The ultraviolet-visible (UV–vis) spectra of CuO@PDA@AuNPs exhibited partial overlap with ECL spectra of Ce(III, IV)-MOF@Ru, thus efficiently initiating the ECL-RET interaction between the donor and acceptor. With the purpose of demonstrating the superiority of newly obtained self-enhanced nanoemitter and donor-acceptor couple, an ECL immunoassay was proposed for the analysis of HER2 with range of 0.2 fg/mL ~ 10 ng/mL and the limit of detection of 0.067 fg/mL. Therefore, this method supplies convenient and significant strategy for the clinical analysis.

1. Introduction

Electrochemiluminescent (ECL), as a prospective technology with outstanding controllability, perfect sensitivity, broad detection range and simple instruments has attracted considerable interest and displays extensive applications for the bioanalysis [1–3]. Among numerous ECL analytical strategies, it is essential to actively search for or create ECL emitters with admirable efficiency, such as $Ru(bpy)_3^{2+}$ [4,5], luminol [6,7] and nanomaterials [8,9]. $Ru(bpy)_3^{2+}$ is one of the most widespread investigated electrochemiluminophores, which has been prosperously commercialized owing to the admirable ECL performance with high stability among water-soluble circumstances [10,11]. However, in view of the perfect water-solubility of $Ru(bpy)_3^{2+}$, it was generally difficult to utilize it for the biosensing platform of solid type. Many attempts have been implemented to assemble $Ru(bpy)_3^{2+}$ on carrier materials that possess desirable properties, for example the high specific surface area, excellent electroconductibility and biocompatibility [12,13]. Considering these demands, it is still significant to explore suitable materials

* Corresponding author.
** Corresponding author at: Collaborative Innovation Center for Green Chemical Manufacturing and Accurate Detection, School of Chemistry and Chemical Engineering, University of Jinan, Jinan 250022, PR China.
E-mail addresses: chm_liuxj@ujn.edu.cn (X. Liu), sdjndxwq@163.com (Q. Wei).

https://doi.org/10.1016/j.snb.2024.136905
Received 6 September 2024; Received in revised form 26 October 2024; Accepted 5 November 2024
Available online 6 November 2024

for encapsulating the $Ru(bpy)_3^{2+}$ luminescent molecules.

Metal-organic frameworks (MOFs) are innovative and highly outstanding porous nanomaterials along with precisely definable crystalline nanostructure, great superficial area, and impressive capability to accommodate various agents, which have attracted significant attention [14–16]. At present, owing to the remarkably excellent structure, MOFs have been utilized as the host materials to assemble a series of luminophores, such as $Ru(bpy)_3^{2+}$ [12], nanoclusters [17], and quantum dots [18]. Although previous studies have mainly investigated the ECL behaviors of these luminophores with MOF utilized as carriers, there have been no reports about MOFs serving as both encapsulant for incorporating luminophores and accelerator for coreactant. However, it is not difficult to achieve the above purpose based on the perfect nanostructure of MOFs. Fortunately, the Ce-based MOFs (Ce(III, IV)-MOF) possesses substantial metal active sites owing to its distinctive three-dimensional (3D) infinite extension framework structure, and controllable porosity, making it a suitable hosts for luminescent molecules [19,20]. Nevertheless, the exploration of utilizing Ce-based MOFs compound as a coreaction accelerator for tripropylamine (TPrA) is still in the early stages. Hence, this is not difficult to achieve on account of the exceptional redox reversibility of Ce^{3+}/Ce^{4+}, allowing for recycling through electrochemical redox reactions.

Taking the above-mentioned advantages into consideration, Ce(III, IV)-MOF diaplayed admirable catalytic activity, which could prominently activate TPrA to generate substantial radicals. Meanwhile, the $Ru(bpy)_3^{2+}$ were trapped within 3D infinite extension framework Ce(III, IV)-MOF that contained cage structures. As a result, a self-enhanced emitter of Ce(III, IV)-MOF@Ru is created, which efficiently reduces the distance of electron transmission and minimizes the loss of energy, prominently enhancing the ECL efficiency. Meanwhile, polydopamine (PDA), a biocompatible, innocuous, and admire polymer has fulfilled the requirements of bioanalysis [21,22]. The unique chemical composition of PDA includes multiple surface-functionalized groups. The catechol construction of PDA can be readily oxidized to obtain the o-benzoquinone, leading to the suppression of ECL response [23]. Additionally, the gold nanoparticles (AuNPs) possess the excellent electrical conductivity and biocompatibility [24]. Thus, benefitting from the excellent characteristics of this developed Ce(III, IV)-MOF@Ru and CuO@PDA@AuNPs, a novel donor-acceptor pair that relies on resonance energy transfer (RET) [25] among them has been successfully created for the first time. Furthermore, there has been a significant overlapping among the ECL spectra of Ce(III, IV)-MOF@Ru and ultraviolet-visible (UV–vis) spectra of CuO@PDA@AuNPs [23]. With the aim of preserving the bioactivity of incubated antibodies, the site-oriented approach utilizing HWRGWVC (HWR) [26,27], a heptapeptide with the capability for selectively capturing the Fc segment of the antibodies, was employed on the surface of Ce(III, IV)-MOF@Ru and CuO@PDA@AuNPs. This site-oriented method has been previously shown to enhance the incubation efficiency and maintain the bioactivity of the antibodies better than conventional methods, as demonstrated in our previous research [28]. Benefitting from the above superiorities, a successful development of a sandwich-type ECL biosensor has been achieved. In this biosensor, Ce(III, IV)-MOF@Ru-HWR-Ab_1 serves as the sensing platform and ECL indicator, while CuO@PDA@AuNPs-HWR-Ab_2 as the RET acceptor. With the purpose of offering an admire technique for early test of breast cancer, the selected analyte was the human epidermal growth factor receptor-2 (HER2) [29]. The HER2 could serve a significant clinical monitoring and prognostic indicator and is also a key target for selecting tumor targeted therapy drugs [30]. Then, the biosensor displayed a satisfactory linear response within the concentration ranging from 0.2 fg/mL to 10 ng/mL and attained an impressive detection limit of 0.067 fg/mL.

2. Experimental

2.1. Chemicals, materials and apparatus

The chemicals, materials and apparatus, and synthesis of Ce (III, IV)-MOF@Ru-HWR and CuO@PDA@AuNPs-HWR-Ab_2 are exhibited in the Supporting Information.

2.2. Fabrication of the constructed ECL immunosensor

The prepared procedure for this immunosensor was displayed in Scheme 1C. The bare glassy carbon electrode (GCE) was primary polished with Al_2O_3 powder and cleaned via ultrapure water, next dried through N_2. Then, 10 μL of Ce(III, IV)-MOF@Ru-HWR (2 mg/mL) was covered on GCE and cleaned by 0.1 mol/L phosphate buffered saline (PBS, pH 7.4) slightly. Next, 10 μL of as-proposed Ab_1 (10 μg/mL) was modified onto the Ce(III, IV)-MOF@Ru-HWR surface and kept at 4 °C for 1 h, and 3 μL of bovine serum albumin (BSA) (1 wt%) was modified on the surface of electrode to seal nonspecific binding sites. Then, 10 μL of diverse contents of HER2 were decorated onto electrode surface and maintained at 37 °C for 1 h. Eventually, 10 μL of CuO@PDA@AuNPs-HWR-Ab_2 bioconjugate was linked to HER2 for completing the biosensor construction.

2.3. Electrochemical and ECL analysis

Cyclic voltammetry (CV) and ECL technique were separately employed to obtain their measurements. The corresponding ECL experiments were conducted in the 0.1 mol/L PBS (pH 7.4) with 10 mmol/L TPrA. Meanwhile, the conditions of this experiment included the photomultiplier tube voltage of 800 V, the scanning voltage from 0 to +1.6 V at the rate of 0.1 V/s.

3. Results and discussion

3.1. Characterizations of Ce(III)-MOF, Ce(III, IV)-MOF and Ce(III, IV)-MOF@Ru

As displayed in Fig. 1A, the X-ray diffraction (XRD) of Ce(III)-MOF was accordant with preceding researches and could be indexed to the Ce-BTC [20,31]. Upon the introduction of NaOH with H_2O_2 for sectional oxidation, this acquired Ce(III)-MOF revealed a shift in its peak in the XRD pattern. This shift can be attributed to the alteration of crystalline construction caused by intense oxidized reaction, implying the presence of Ce(III) residue. Simultaneously, the occurrence of distinct peaks corresponded to the cubic morphology of CeO_2 (JCPDS 34–0394), confirming the acquisition of Ce(IV) [32]. Upon the Fig. 1B, the XRD of CuO was consistent with previous study and could be attributed to the monoclinic nanostructure [33]. Next, as indicated in the Fig. 1C-D, the average dimension of the rod-like structure exhibited by Ce(III)-MOF was determined to be 500 nm, indicating its uniformity. Following partial oxidized reaction, the conformation for Ce(III, IV)-MOF remained analogous to that of Ce(III)-MOF along with the coarser surface (Fig. 1E). This surface roughness has the potential to enhance the effective surface, consequently promoting the catalytic performance [20]. Meanwhile, as observed in the Fig. 1F, the CuO presented a rough appearance along with the average size of approximately 300 nm. With the purpose of examining the synthesized AuNPs on CuO@PDA surface, the SEM image of CuO@PDA@AuNPs were exhibited in Fig. 1G. The observation revealed that the AuNPs were evenly dispersed on the CuO@PDA surface.

As exhibited in the Fig. 1H-I, the surfacial chemical formations and valence states of elements for the obtained Ce(III, IV)-MOF@Ru nanomaterials were measured by the X-ray photoelectron spectroscopy (XPS). In the Fig. 1H, it revealed the presence of Ce, Ru, and O based on survey spectra. In addition, the high resolution spectra for Ce 3d in the

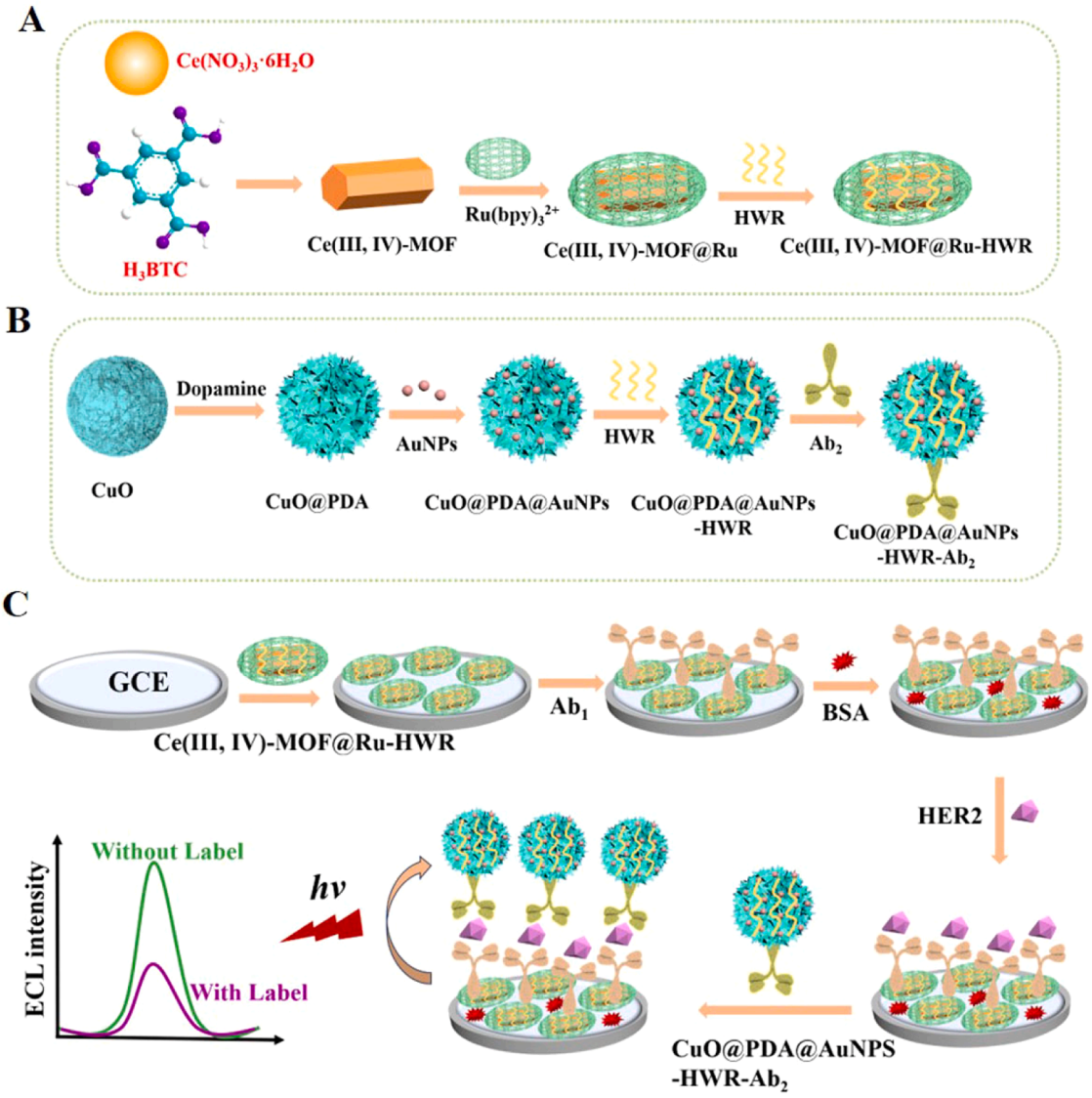

Scheme 1. Preparation of (A) Ce(III, IV)-MOF@Ru-HWR and (B) CuO@PDA@AuNPs-HWR-Ab_2; (C) Fabrication process for the ECL immunosensor.

Fig. 1I demonstrated six evident peaks, corresponding to Ce(III) and Ce (IV), respectively.

3.2. *ECL response amplification mechanism of Ce(III, IV)-MOF@Ru and the quenching mechanism of CuO@PDA@AuNPs*

According to the aforementioned experimental process, the Ce(III)-MOF was oxidated by NaOH and H_2O_2 to obtain Ce(III, IV)-MOF. In the Fig. 2A-B, Ce^{3+} and Ce^{4+} were coexisted inside the Ce(III, IV)-MOF nanostructure. Furthermore, the possible mechanisms for ECL in the constructed immunosensor were exhibited in the Fig. 2C-D. When TPrA was used as the coreactant of the Ce(III)-MOF@Ru system, $TPrA^{\bullet+}$ was formed around the electrode, resulting in an excellent ECL signal. Subsequently, as Ce(III, IV)-MOF@Ru participated into the ECL formed process, the generation of $TPrA^{\bullet+}$ was distinctly increased, acquiring obvious ECL intensity amplification.

The important function of Ce(III, IV)-MOF in the Ce(III, IV)-MOF@Ru/TPrA system was investigated. As displayed in Fig. 3A-B, the investigations on the behaviors of simultaneous ECL and CV measurements upon various circumstances were demonstrated. No ECL signal has been obtained from GCE (Fig. 3 A, curve a) in PBS (pH 7.4) including TPrA. Subsequently, under the modification of Ce (III)-MOF (1 mg/mL) and Ce (III, IV)-MOF (1 mg/mL) onto the GCE, no ECL intensities were also displayed (curve b and c), which demonstrated that the Ce (III)-MOF and Ce (III, IV)-MOF could not generate ECL response. Similarly, when the identical content of Ce(III)-MOF@Ru and Ce(III, IV)-MOF@Ru were modified onto GCE, obvious ECL intensities of 16625 a.u. and 22017 a.u. were acquired (curve d and e). Moreover, the ECL response for Ce(III, IV)-MOF@Ru was more stronger than Ce(III)-MOF@Ru, which indicated the ECL response was increased by the Ce(III, IV)-MOF. On account of the coreactant ECL reaction mechanism and existing literature, it has been proven that Ce(III, IV)-MOF could serve as the successful coreaction accelerator for the system [28,34,35], which could improve the generation of the radicals intermediate to obtain the enhanced ECL response. In addition, by effectively reducing the electron transfer distance and generating a highly oxidizing species, the self-enhanced emitter of Ce(III, IV)-MOF@Ru could facilitate the oxidized reaction of coreactant TPrA and enhanced the ECL efficiency. Moreover, the ECL emission potential of Ce(III, IV)-MOF@Ru was more positive than the Ce(III)-MOF@Ru, and the current was the strongest, which indicated that Ce(III, IV)-MOF took a significant part in enhancing the transfer of electron. Then, the possible ECL mechanism was displayed as follows (Eqs. 1–5).

$$TPrA - e^{-} \longrightarrow (Ce(III, IV)\text{-}MOF)\ TPrA^{\bullet+}\ (\textbf{more}) \quad (1)$$

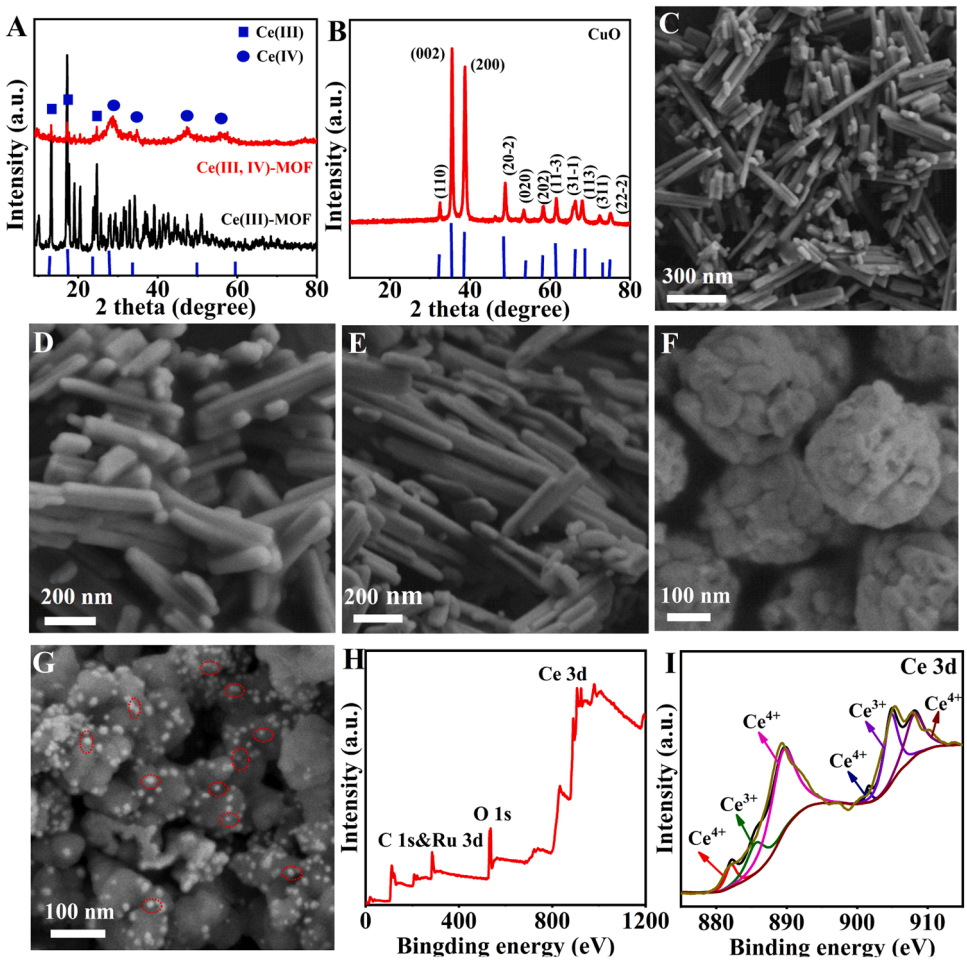

Fig. 1. XRD patterns for (A) Ce(III)-MOF (a) and Ce(III, IV)-MOF (b), and (B) CuO. SEM images of Ce(III)-MOF (C and D). SEM images of (E) Ce(III, IV)-MOF, (F) CuO and (G) CuO@PDA@AuNPs. (H) XPS survey spectra for Ce(III, IV)-MOF@Ru, and the high resolution spectra of Ce 3d (I) for Ce(III, IV)-MOF@Ru.

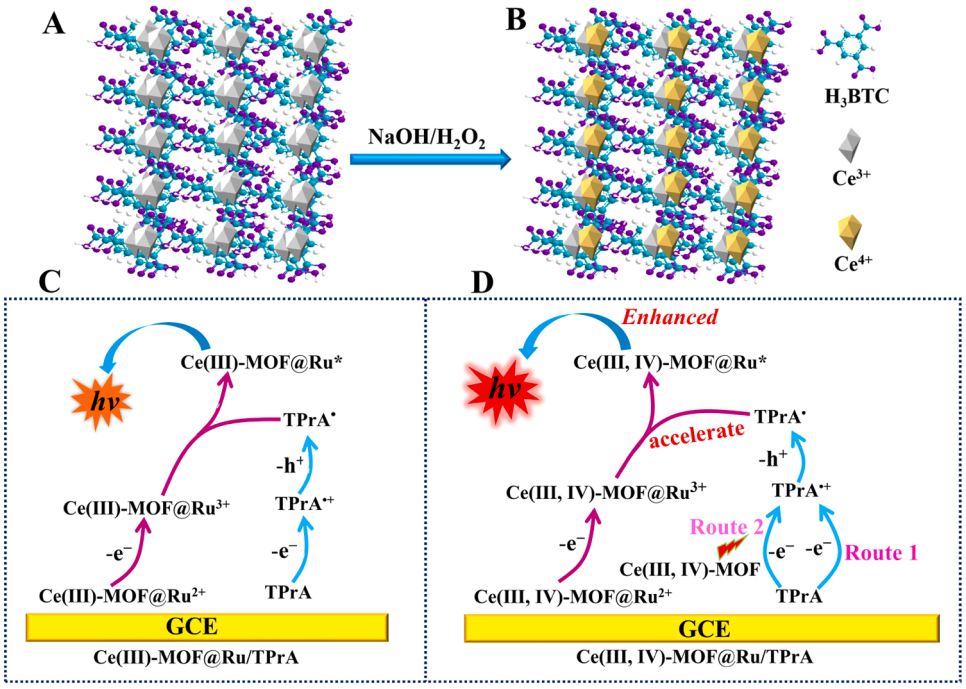

Fig. 2. (A) The synthesis diagram of the Ce(III, IV)-MOF (B) from Ce(III)-MOF (A). Mechanistic illustrations of (C) Ce(III)-MOF@Ru/TPrA and (D) Ce(III, IV)-MOF@Ru/TPrA system.

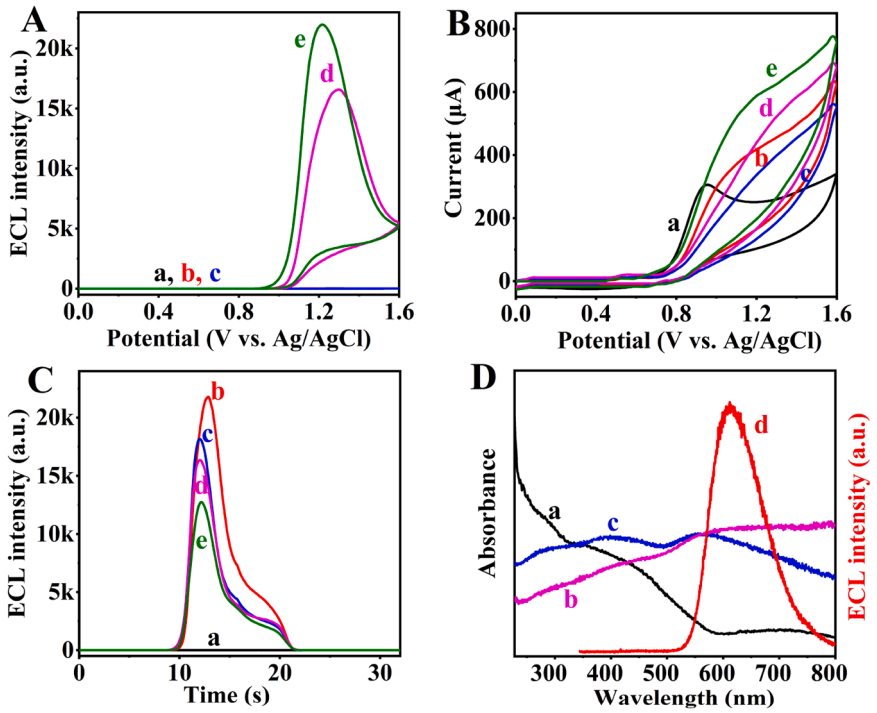

Fig. 3. (A) ECL response-potential and (B) CV curves for (a) GCE, (b) Ce(III)-MOF/GCE, (c) Ce(III, IV)-MOF/GCE, (d) Ce(III)-MOF@Ru/GCE and (e) Ce(III, IV)-MOF@Ru/GCE inside 0.1 mol/L PBS with 10 mmol/L TPrA. (C) ECL intensity of (a) GCE, (b) Ce(III, IV)-MOF@Ru/GCE, (c) CuO/Ce(III, IV)-MOF@Ru/GCE, (d) CuO@PDA/Ce(III, IV)-MOF@Ru/GCE, and (e) CuO@PDA@AuNPs/Ce(III, IV)-MOF@Ru/GCE inside 0.1 mol/L PBS with 10 mmol/L TPrA. (D) UV−vis absorption of (a) CuO, (b) CuO@PDA and (c) CuO@PDA@AuNPs; the ECL emission spectra of (d) Ce(III, IV)-MOF@Ru.

$$TPrA^{\bullet+} \longrightarrow TPrA^{\bullet} + H^{+} \quad (2)$$

$$Ru(bpy)_3^{2+} - e^{-} \longrightarrow Ru(bpy)_3^{3+} \quad (3)$$

$$Ru(bpy)_3^{3+} + TPrA^{\bullet} \longrightarrow Ru(bpy)_3^{2+*} + \text{product} \quad (4)$$

$$Ru(bpy)_3^{2+*} \longrightarrow Ru(bpy)_3^{2+} + h\nu \quad (5)$$

Meanwhile, the sensitivity of immunosensor was also significantly affected by the efficiency of quenching probe [36]. With the purpose of investigating quenching behavior of CuO@PDA@AuNPs, these quenching nanomaterials of CuO, CuO@PDA and CuO@PDA@AuNPs were synthesized, separately. As displayed in the Fig. 3 C, no signal was generated from GCE (curve a), but the Ce(III, IV)-MOF@Ru displayed an obvious ECL intensity (curve b). When CuO was decorated onto the Ce (III, IV)-MOF@Ru surface, a noticeable reduction in ECL emission (curve c) was observed, which could be obtained that CuO possessed the ability to weaken ECL emission of Ce(III)-MOF@Ru via energy transduction. When CuO@PDA was decorated onto the above surface (curve d), a weaker ECL intensity was achieved, which was due to the inhibitory effect of PDA loaded by the CuO nanoparticles. This was because the interaction between the catechol or benzoquinone in PDA with CuO to the excited status of Ce(III, IV)-MOF@Ru, leading to energy transfer and quenching [6,23]. Next, when CuO@PDA@AuNPs was decorated onto Ce(III, IV)-MOF@Ru surface, the ECL intensity was the least, certifying that both CuO@PDA and AuNPs would quench ECL response of Ce (III)-MOF@Ru. As revealed in the curve e of Fig. 3 C, the CuO@PDA@AuNPs complex exhibited the highest level of quenching intensity towards the ECL response of Ce(III)-MOF@Ru emitter through the energy transfer.

With the aim of exploring the potential quenching mechanism of CuO@PDA@AuNPs toward Ce(III, IV)-MOF@Ru, the UV−vis spectra for CuO, CuO@PDA and CuO@PDA@AuNPs and the ECL spectrum for Ce (III, IV)-MOF@Ru were measured (Fig. 3D). From the observation, it could be inferred that there was a partial overlap between ECL spectra of Ce(III, IV)-MOF@Ru (curve d) and UV–vis of CuO (curve a), which suggested the potential presence of ECL-RET. Next, the ECL signal of Ce (III, IV)-MOF@Ru was also quenched via CuO@PDA, and then the mechanism may be based on the existence of substantial functional groups of catechol or benzoquinone on the surface of CuO@PDA, which quenched the ECL signals. The findings demonstrated that the ECL spectrum for Ce(III, IV)-MOF@Ru spanning from approximately 500 nm to 800 nm (curve d). Meanwhile, the UV–vis spectra for CuO@PDA@AuNPs displayed a wide absorption extent. A distinct spectral overlap was detected between the ECL spectrum of Ce(III, IV)-MOF@Ru and the UV–vis spectrum of CuO@PDA@AuNPs, thus indicating the feasibility of RET between Ce(III, IV)-MOF@Ru (energy donor) and CuO@PDA@AuNPs (energy acceptor).

3.3. *Feasibility of the ECL immunosensing*

The successive property of immunosensor was obtained by electrochemical impedance spectroscopy (EIS). In the Fig. 4 A, the achieved GCE revealed a little semicircle (curve a), which was owing to the transfer of free-electron. The Ce(III, IV)-MOF@Ru-HWR/GCE showed a little semicircle (curve b), resulting from perfect conductivity of Ce(III, IV)-MOF@Ru. After Ab_1 was coated on the electrode (curve c), the semicircle increased, which was based on an impediment for electron transfer. Then, with the sequent decoration of BSA and HER2 (curve d and e), the resistance enlarged, successively. Finally, the resistance further increased by the decoration of CuO@PDA@AuNPs- HWR-Ab_2 bioconjugates (curve f), which demonstrated the perfect fabrication of immunosensor. In addition, as exhibited in the Fig. 4B, the CV was also an electrochemical manner for testing the fabricated procedure of immunosensor. The obtained less and less peak value along with enhanced peak potential separation was observed after successive decoration onto the electrode, indicating the hindrance for the transfer of electron and best modification of the proposed immunosensor.

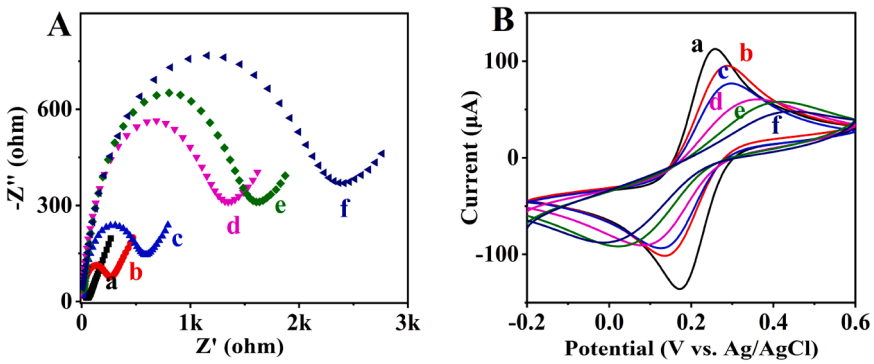

Fig. 4. (A) EIS and (B) CV profiles for step-by-step decorated electrodes inside 0.1 mol/L PBS including 5 mmol/L $Fe(CN)_6^{3-/4-}$: (a) GCE, (b) Ce(III, IV)-MOF@Ru-HWR/GCE, (c) Ab_1/Ce(III, IV)-MOF@Ru-HWR/GCE, (d) BSA/Ab_1/Ce(III, IV)-MOF@Ru-HWR/GCE, (e) HER2/BSA/Ab_1/Ce(III, IV)-MOF@Ru-HWR/GCE and (f) CuO@PDA@AuNPs-HWR-Ab_2/HER2/BSA/Ab_1/Ce(III, IV)-MOF@Ru-HWR/GCE.

3.4. Optimization of the experimental conditions

The appropriate circumstance of pH was vital to the proposed immunosensor. After studying the compatibility of obtained immunosensor to various pH value from 6.0 to 8.5, the neutral circumstances (pH 7.4) was selected for subsequent research as displayed in the Fig. S1A. TPrA has been acted as a coreactant for Ce(III, IV)-MOF@Ru and the content of TPrA was optimized as shown in Fig. S1B. It was discovered that the signal acquired the best result when the TPrA content was 10 mmol/L. Furthermore, the ECL response enhanced when the content of Ce(III, IV)-MOF@Ru was below 1.0 mg/mL, and then reduced when the content exceeded 1 mg/mL (Fig. S1C). Hence, 1 mg/mL of Ce (III, IV)-MOF@Ru was applied in the ECL system. The reaction time for Ab_2 bioconjugates was displayed in Fig. S1D, and this consequence demonstrated the best time of 60 min. The reaction time for Ab_2 bioconjugates was less compared to other ways, which was based on site-oriented modification of antibodies through HWR.

3.5. Analytical performance of the ECL signal-off strategy in HER2 determination

With the purpose of estimating the analytical property of the fabricated biosensing strategy, ECL signals of this immunosensor towards different HER2 contents were achieved upon the optimal status. As displayed in the Fig. 5 A, the ECL signal diminished sequentially while the content of HER2 improved from 0.2 fg/mL to 10 ng/mL. Furthermore, the Fig. 5B revealed the relevant linear relationship of ECL signal and the logarithm of HER2 content (lg *c*) along with linear equation of $Y = -1520.9 \lg c + 8474.0$ and relevant correlation coefficient of 0.998. Then, the limit of detection (LOD) of constructed immunosensor was 0.067 fg/mL, exhibiting better sensitivity than other prevenient researches (Table S1).

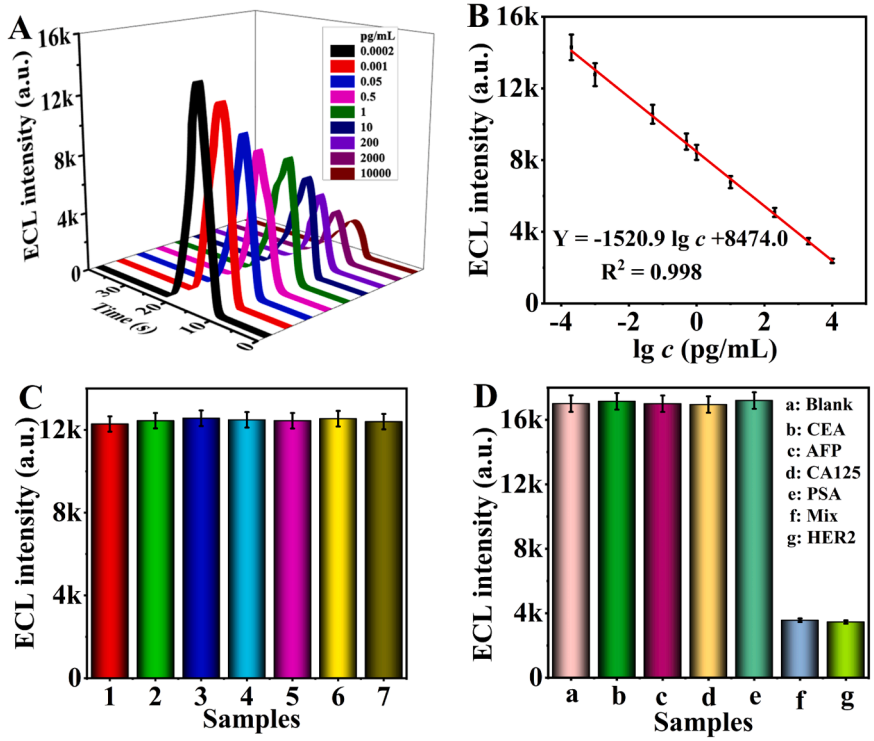

Fig. 5. (A) ECL response-time profiles and (B) relevant calibration curve for this immunosensor to diverse contents of HER2 (from 0.2 fg/mL to 10 ng/mL) inside 0.1 mol/L PBS (pH 7.4) containing 10 mmol/L TPrA. (C) reproducibility of proposed immunosensor to HER2. (D) selectivity of proposed immunosensor to 2 ng/mL HER2 and 200 ng/mL other interferences. Error bars = SD (n = 3).

3.6. Reproducibility, selectivity and stability of the constructed immunosensor

With the aim of evaluating reproducibility, seven prepared electrodes were firstly measured to indicate the perfect reproducibility with the obtained relative standard deviation (RSD) of 1.6 % (Fig. 5 C). As displayed in Fig. 5D, carcinoembryonic antigen (CEA), α-fetoprotein (AFP), carcinoma antigen 125 (CA125) and prostate specific antigen (PSA) have been selected as interfering materials, and the mixture included above proteins and HER2. The interfering proteins were with the content 100-folds of the HER2. All results indicated that although the concentrations of interfering materials were 100 times higher than the target analyte, the proposed immunoassay model could accurately distinguish and detect the target analyte, which demonstrated the perfect selectivity of the recommended immunoassay strategy. Meanwhile, the stability was tested through reserving the achieved immunosensor for two weeks, which displayed the ECL intensity of 92 % the primary intensity, certifying the favorable stability.

3.7. Analysis of HER2 in human serum samples

The approval of constructed ECL immunosensor was further testified through measuring the consequences for ECL immunoassay to HER2 detection in the serum samples. Next, the standard addition method was utilized for achieving relevant determination. The obtained results have been revealed in Table S2**,** which displayed the results of RSD from 2.24 % to 3.31 %, and the recovery from 98.1 % to 102.4 %, indicating well performance for the proposed method in the clinical application.

4. Conclusion

In brief, the study prepared a self-enhanced emitter with Ce(III, IV)-MOF efficiently immobilized with $Ru(bpy)_3^{2+}$ to achieve Ce(III, IV)-MOF@Ru, and CuO@PDA@AuNPs as the perfect quencher in this ECL immunosensor for ultrasensitive determination of HER2. By virtue of its high coreaction accelerated activity, the Ce(III, IV)-MOF has the capacity to stimulate TPrA and generate a substantial quantity of radicals, leading to a robust and consistent ECL signal. Meanwhile, the obtained CuO@PDA@AuNPs could effectively quench the ECL response of Ce(III, IV)-MOF@Ru, attributing to the partial spectra overlap between Ce(III, IV)-MOF@Ru and CuO@PDA@AuNPs for triggering the ECL-RET phenomenon. Additionally, the surface of CuO@PDA@AuNPs contained massive functional groups, inhibiting the ECL response. Consequently, the multiple quenching of CuO@PDA@AuNPs for the ECL response was obtained, which efficiently promoted sensitivity of immunosensor. Significantly, this work offers novel concepts through utilizing Ce(III, IV)-MOF for both encapsulant and coreaction accelerator in biosensors.

CRediT authorship contribution statement

Huangxian Ju: Project administration. **Xuejing Liu:** Writing – review & editing, Formal analysis. **Qin Wei:** Writing – review & editing, Project administration, Funding acquisition. **Nuo Zhang:** Writing – review & editing. **Hongying Jia:** Writing – original draft, Data curation, Conceptualization. **Yuyang Li:** Writing – review & editing. **Dan Wu:** Supervision. **Hongmin Ma:** Formal analysis.

Declaration of Competing Interest

The authors declare that they have no known competing financial interests or personal relationships that could have appeared to influence the work reported in this paper.

Acknowledgements

This project was supported by the National Natural Science Foundation of China (22304060 and 22274062), the Natural Science Foundation of Shandong Province (ZR2023QB019), and the China Postdoctoral Science Foundation (2023M741359).

Appendix A. Supporting information

Supplementary data associated with this article can be found in the online version at doi:10.1016/j.snb.2024.136905.

Data availability

No data was used for the research described in the article.

References

[1] Y.G. Wang, G.H. Zhao, H. Chi, S.H. Yang, Q.F. Niu, D. Wu, W. Cao, T.D. Li, H. M. Ma, Q. Wei, Self-luminescent lanthanide metal-organic frameworks as signal probes in electrochemiluminescence immunoassay, J. Am. Chem. Soc. 143 (2021) 504–512.
[2] N.N. Wang, H. Gao, Y.Z. Li, G.M. Li, W.W. Chen, Z.C. Jin, J.P. Lei, Q. Wei, J.H. Xian, Dual intramolecular electron transfer for in situ coreactant-embedded electrochemiluminescence microimaging of membrane protein, Angew. Chem. Int. Ed. 60 (2020) 197–201.
[3] H.Y. Jia, L. Yang, X. Dong, L.M. Zhou, Q. Wei, H.X. Ju, Cysteine modification of glutathione-stabilized Au nanoclusters to red-shift and enhance the electrochemiluminescence for sensitive bioanalysis, Anal. Chem. 94 (2022) 2313–2320.
[4] W.Q. Bai, A.P. Cui, M.Z. Liu, X. Qiao, Y. Li, T. Wang, Signal-off electrogenerated chemiluminescence biosensing platform based on the quenching effect between ferrocene and $Ru(bpy)_3^{2+}$-functionalized metal-organic frameworks for the detection of methylated RNA, Anal. Chem. 91 (2019) 11840–11847.
[5] M.M. Xia, F. Zhou, X.Y. Feng, J.H. Sun, L. Wang, N. Li, X.Y. Wang, G.F. Wang, A DNAzyme-based dual-stimuli responsive electrochemiluminescence resonance Energy transfer platform for ultrasensitive anatoxin-a detection, Anal. Chem. 93 (2021) 11284–11290.
[6] W.J. Lai, J.J. Li, M.Z. Jiang, P.L. Li, M. Wang, C.Y. Ma, C.L. Zhao, Y. Qi, C.L. Hong, Electrochemiluminescence immunosensors based on ECL-RET triggering between Mn SANE/PEI-luminol and PtCu/h-MPF for ultrasensitive detection of CEA, Anal. Chem. 95 (2023) 7109–7117.
[7] J.N. Guo, M.S. Xie, P.Y. Du, Y. Liu, X.Q. Lu, Signal amplification strategy using atomically gold-supported VO_2 nanobelts as a co-reaction accelerator for ultrasensitive electrochemiluminescent sensor construction based on the resonance energy transfer platform, Anal. Chem. 93 (2021) 10619–10626.
[8] L. Fu, X.W. Gao, S.T. Dong, H.Y. Hsu, G.Z. Zou, Surface-defect-induced and synergetic-effect-enhanced NIR-II electrochemiluminescence of Au-Ag bimetallic nanoclusters and its spectral sensing, Anal. Chem. 93 (2021) 4909–4915.
[9] L. Fu, K.N. Fu, X.W. Gao, S.T. Dong, B. Zhang, S.J. Fu, H.-Y. Hsu, G.Z. Zou, Enhanced near-infrared electrochemiluminescence from trinary Ag-In-S to multinary Ag-Ga-In-S nanocrystals via doping-in-growth and its immunosensing applications, Anal. Chem. 93 (2021) 2160–2165.
[10] L. Fu, B. Zhang, K.N. Fu, X.W. Gao, G.Z. Zou, Electrochemically lighting up luminophores at similar low triggering potentials with mechanistic insights, Anal. Chem. 92 (2020) 6144–6149.
[11] D.F. Feng, M.X. Xiao, P.H. Yang, A sensitive electrochemiluminescence urea sensor for dynamic monitoring of urea transport in living cells, Anal. Chem. 95 (2023) 766–773.
[12] G.H. Zhao, Y.G. Wang, X.J. Li, Q. Yue, X. Dong, B. Du, W. Cao, Q. Wei, Dual-quenching electrochemiluminescence strategy based on three-dimensional metal-organic frameworks for ultrasensitive detection of amyloid-beta, Anal. Chem. 91 (2019) 1989–1996.
[13] G.H. Zhao, Y.G. Wang, X.J. Li, X. Dong, H. Wang, B. Du, W. Cao, Q. Wei, Quenching electrochemiluminescence immunosensor based on resonance energy transfer between ruthenium (II) complex incorporated in the UiO-67 metal–organic framework and gold nanoparticles for insulin detection, ACS Appl. Mater. Interfaces 10 (2018) 22932–22938.
[14] J.Y. Cui, X.J. Xu, C.N. Yang, J.J. Wang, Q.F. Guo, G.M. Nie, A difunctional electrochemiluminescence sensor based on Ru-MOFs and strand-displacement-amplification reaction for ultrasensitive detection of Hg^{2+} and Ag^{+}, Sens. Actuators B Chem. 378 (2023) 133141.
[15] C. Doonan, R. Riccò, K. Liang, D. Bradshaw, P. Falcaro, Metal–organic frameworks at the biointerface: synthetic strategies and applications, Acc. Chem. Res. 50 (2017) 1423–1432.
[16] K. Adil, Y. Belmabkhout, R.S. Pillai, A. Cadiau, P.M. Bhatt, A.H. Assen, G. Maurin, M. Eddaoudi, Gas/vapour separation using ultra-microporous metal–organic frameworks: insights into the structure/separation relationship, Chem. Soc. Rev. 46 (2017) 3402–3430.
[17] Y.M. Nie, X.L. Tao, H.W. Zhang, Y.Q. Chai, R. Yuan, Self-assembly of gold nanoclusters into a metal-organic framework with efficient electrochemiluminescence and their application for sensitive detection of rutin, Anal. Chem. 93 (2021) 3445–3451.
[18] D. Du, J. Shu, M. Guo, M.A. Haghighatbin, D. Yang, Z. Bian, H. Cui, Potential-resolved differential electrochemiluminescence immunosensor for crdiac troponin

I based on MOF-5-wrapped CdS quantum dot nanoluminophores, Anal. Chem. 92 (2020) 14113–14121.
[19] Y.H. Xiong, S.H. Chen, F.G. Ye, L.J. Su, C. Zhang, S.F. Shen, S.L. Zhao, Synthesis of a mixed valence state Ce-MOF as an oxidase mimetic for the colorimetric detection of biothiols, Chem. Commun. 51 (2015) 4635–4638.
[20] X.Z. Song, S.Q. Yu, L. Zhao, Y.J. Guo, X. Ren, H.M. Ma, S.F. Wang, C.N. Luo, Y.Y. Li, Q. Wei, Efficient ABEI-dissolved O_2-Ce(III, IV)-MOF ternary electrochemiluminescent system combined with self-assembled microfluidic chips for bioanalysis, Anal. Chem. 94 (2022) 9363–9371.
[21] B. Xing, W.J. Zhu, X.P. Zheng, Y.Y. Zhu, Q. Wei, D. Wu, Electrochemiluminescence immunosensor based on quenching effect of SiO_2@PDA on SnO_2/rGO/Au NPs-luminol for insulin detection, Sens. Actuators B Chem. 265 (2018) 403–411.
[22] T.F. Shi, L.H. Hu, J.Y. Chen, Q.Q. Cui, H. Yu, Y.Y. Li, D. Wu, H.M. Ma, Q. Wei, H. X. Ju, Dual-quenching electrochemiluminescence system based on resonance energy transfer from gold dendrite@polypyrrole core–shell nanoparticles enhanced g-C_3N_4 to ZnONFs@PDA-sCuO for procalcitonin immunosensing, Sens. Actuators B Chem. 371 (2022) 132591.
[23] C. Wang, N. Zhang, D. Wei, R. Feng, D.W. Fan, L.H. Hu, Q. Wei, H.X. Ju, Double electrochemiluminescence quenching effects of Fe_3O_4@PDA-Cu_XO towards self-enhanced $Ru(bpy)_3^{2+}$ functionalized MOFs with hollow structure and it application to procalcitonin immunosensing, Biosens. Bioelectron. 142 (2019) 111521.
[24] H.Y. Jia, P.C. Gao, H.M. Ma, Y.Y. Li, J. Gao, B. Du, Q. Wei, Ultrasensitive electrochemical immunosensor for squamous cell carcinoma antigen detection using lamellar montmorillonite-gold nanostructures as signal amplification, Talanta 132 (2015) 803–808.
[25] G.H. Zhao, Y. Du, N. Zhang, Y. Li, G.Z. Bai, H.M. Ma, D. Wu, W. Cao, Q. Wei, Bimetallic metal-organic frameworks as an efficient capture probe in signal On-Off-On electrochemiluminescence aptasensor for Microcystin-LR detection, Anal. Chem. 95 (2023) 8487–8495.
[26] L. Yang, D.W. Fan, Y. Zhang, C.F. Ding, D. Wu, Q. Wei, H.X. Ju, Ferritin-based electrochemiluminescence nanosurface energy transfer system for procalcitonin detection using HWRGWVC heptapeptide for site-oriented antibody immobilization, Anal. Chem. 91 (2019) 7145–7152.
[27] X.Z. Song, X.R. Shao, L. Dai, D.W. Fan, X. Ren, X.J. Sun, C.N. Luo, Q. Wei, Triple amplification of 3,4,9,10-perylenetetracarboxylic acid by Co^{2+}-based metal-organic frameworks and silver-cysteine and its potential application for ultrasensitive assay of procalcitonin, ACS Appl. Mater. Interfaces 12 (2020) 9098–9106.
[28] H.Y. Jia, J.S. Li, L. Yang, D.W. Fan, X. Kuang, X. Sun, Q. Wei, H.X. Ju, Hollow double-shell $CuCo_2O_4$@Cu_2O heterostructures as a highly efficient coreaction accelerator for amplifying NIR electrochemiluminescence of gold nanoclusters in immunoassay, Anal. Chem. 94 (2022) 7132–7139.
[29] X.N. Liu, X.Y. Zhang, R. Feng, X. Ren, D. Wu, X.J. Liu, L. Liu, Q. Wei, Microfluidic immunosensor platform for sensitive detection of human epidermal growth factor receptor-2 based on enhanced cathode electrochemiluminescence of bimetallic nanoclusters, Anal. Chem. 96 (2024) 8390–8398.
[30] D.Q. Leng, Z. Yu, J.J. Liu, W.H. Jin, T. Wu, X. Ren, H.M. Ma, D. Wu, H.X. Ju, Q. Wei, Multifunctional supramolecular hydrogel modulated heterojunction interface carrier transport engineering facilitates sensitive photoelectrochemical immunosensing, Anal. Chem. 96 (2024) 8814–8821.
[31] G.Z. Chen, Z.Y. Guo, W. Zhao, D.W. Gao, C.C. Li, C. Ye, G.X. Sun, Design of porous/hollow structured ceria by partial thermal decomposition of Ce-MOF and selective etching, ACS Appl. Mater. Interfaces 9 (2017) 39594–39601.
[32] J.J. He, Y.H. Xu, W. Wang, B. Hu, Z.J. Wang, X. Yang, Y. Wang, L.W. Yang, Ce(III) nanocomposites by partial thermal decomposition of Ce-MOF for effective phosphate adsorption in a wide pH range, Chem. Eng. J. 379 (2020) 122431.
[33] J.T. Zhang, J.F. Liu, Q. Peng, X. Wang, Y.D. Li, Nearly monodisperse Cu_2O and CuO nanospheres: preparation and applications for sensitive gas sensors, Chem. Mater. 18 (2006) 867–871.
[34] X.Z. Song, L. Zhao, N. Zhang, L. Liu, X. Ren, H.M. Ma, X. Kuang, Y.Y. Li, C.N. Luo, Q. Wei, Ultrasensitive electrochemiluminescence biosensor with silver nanoclusters as a novel signal Probe and alpha-Fe_2O_3-Pt as an efficient co-reaction accelerator for procalcitonin immunoassay, Anal. Chem. 95 (2023) 1582–1588.
[35] L. Zhao, X.Z. Song, X. Ren, D.W. Fan, Q. Wei, D. Wu, Rare self-luminous mixed-valence Eu-MOF with a self-enhanced characteristic as a near-infrared fluorescent ECL probe for nondestructive immunodetection, Anal. Chem. 93 (2021) 8613–8621.
[36] G.H. Zhao, X. Dong, Y. Du, N. Zhang, G.Z. Bai, D. Wu, H.M. Ma, Y.G. Wang, W. Cao, Q. Wei, Enhancing electrochemiluminescence efficiency through introducing atomically dispersed ruthenium in nickel-based metal-organic frameworks, Anal. Chem. 94 (2022) 10557–10566.

Hongying Jia received her Ph.D. degree from China University of Jinan (Jinan China) in 2022. Her main research interests are the preparation of nano-luminescence materials, electrochemiluminescence biosensor technology, and their application.

Nuo Zhang received her Ph.D. degree in chemical engineering and technology from Shandong University of Technology, Zibo, China. Now, she is a senior experimentalist at University of Jinan. Her main research interests are electrochemical biosensors and photoelectrochemical biosensors.

Yuyang Li received his Ph.D. degree from China University of Petroleum (East China) in 2018. His main research interest are the design and preparation of functional nanomaterial, sensor technology, fluorescence imaging, and their industrial application.

Hongmin Ma received Ph.D. degree from Shandong University (Jinan China). He is now an associate professor at Jinan University. He is mainly engaged in the preparation, properties and applications of porous structures of nanocomposites in sensing analysis.

Dan Wu a professor and received the Ph.D. from Shandong University in 2007. She is a professor at Jinan University. Her research interests include cell imaging analysis, disease markers, food and environmental contaminant analysis, fluorescence and electrochemical biosensing, and energy catalysis.

Xuejing Liu received her Ph.D. degree in Dalian University of Technology in 2015. From 2015–2018, she worked as a postdoctoral fellow in Dalian Institute of Chemical Physics. Afterwards, she began working in University of Jinan. At present, her main research interests are the electrocatalytic conversions and electrochemical biosensors.

Huangxian Ju received his BS, MS and Ph.D. degrees from Nanjing University during 1982–1992. He was a postdoc in Montreal University (Canada) from 1996 to 1997 and a guest professor in three universities of Germany and Ireland in 1999–2000. He became an associate and full professor of Nanjing University in 1993 and 1999. He is currently the director of State Key Laboratory of Analytical Chemistry for Life Science. His research interests focus on analytical biochemistry, biosensing and molecular diagnosis. He has published 13 books and 790 papers in different journals with SCIE h-index of 100 (>38,000 citations) and Google Scholar h-index of.110 (> 44,000 citations).

Qin Wei, a professor and DSc, has devoted herself to analytical teaching and scientific research. She is mainly engaged in the research of disease marker analysis, food analysis, environmental pollutant analysis and treatment, new energy materials and catalytic applications. She has published 710 SCI papers in J. Am. Chem. Soc, Adv. Mater., Adv. Funct. Mater., Anal. Chem., Nano Energy, Biomaterials, J. Mater. Chem. A, Nano Res., Chem. Commun., Biosens. Bioelectron., Carbon, ACS Appl. Mater. Interfaces and other international high-level academic journals and Google Scholar hindex of 84.